Study on blind band elimination in jitter estimation

Haiqiu Liu (刘海秋)[1,2], Dong Wang (王 栋)[1], Dejie Yan (闫得杰)[1], and Shuyan Xu (徐抒岩)[1*]

[1]*Changchun Institute of Optics, Fine Mechanics and Physics, Chinese Academy of Sciences, Changchun 130033, China*

[2]*Graduate University of Chinese Academy of Sciences, Beijing 100049, China*

[*]*Corresponding author: xusy@ciomp.ac.cn*

Received May 7, 2014; accepted July 16, 2014; posted online September 28, 2014

We propose a blind spot elimination method based on an improved layout of CCD in spacecraft jitter estimation. At least three CCDs are required and designed with two pairs of overlapping area and one non-overlapping pair. The two number of lines in space of overlapping pairs are made coprime to minimize the number of common blind spots. The third non-overlapping pair is arranged with the space less than the quotient of the least line frequency and bandwidth. It is used to eliminate the aliasing blind frequencies of the first two overlapping pairs. Experimental results prove the effectiveness of the blind band elimination.

OCIS codes: 120.0120, 120.0280, 120.1880, 280.0280.

doi: 10.3788/COL201412.101203.

Time-delay integration (TDI) push-broom imaging CCD is widely used for high-resolution space cameras, it builds a line-by-line image as the spacecraft flies over the surface of Earth or other planets[1]. Due to the physical housing of each CCD, two adjacent CCDs are usually configured in two rows and overlapping on the edge to obtain images with continuous content[2]. The image pairs captured by the overlapping areas have the same content and are usually used for some high-accuracy measurement applications. The High Resolution Imaging Science Experiment on the Mars Reconnaissance Orbiter detects jitter using the overlapping CCD[1–5]. The Lunar Reconnaissance Orbiter Camera-Narrow Angle Camera flying onboard the Lunar Reconnaissance Orbiter uses the overlapping images for spacecraft jitter assessment[6,7]. The Advanced Spaceborne Thermal Emission and Reflection Radiometer (ASTER) on the Terra Earth Observing System AM-1 spacecraft detects the attitude fluctuation using the overlapping ASTER/short wave infrared imageries[8,9]. Zaunick *et al.*[10–13] used the overlapping images to estimate image motion by an auxiliary matrix image sensor on focal plane.

We take the jitter estimation as an example in the following discussion: jitter estimation method based on the overlapping image pairs possesses a high accuracy and a wide measurement bandwidth, but not all frequencies can be measured by this approach. In order to eliminate the blind spots, we propose a blind spot elimination method based on improved layout of overlapping CCD pairs.

The "jitter" in the jitter estimation means the motion with periods larger than integration time. For an N-line TDI-CCD camera, the integration time equals the product of imaging line time and N. All frequencies cause image smear, but only the jitter with periods larger than the integration time can lead to image geometric distortions, and this jitter is the measured object in jitter estimation[1].

Jitter distorts an image by causing relative motion between a focal plane and imaging positions of ground objects. The relative motion is decomposed into two components in cross-track and down-track directions, $j_x(t)$ and $j_y(t)$, and the corresponding jitter velocities are Δv_x and Δv_y. Images captured by overlapping CCD pairs are used to estimate jitter. Figure 1 shows the imaging process of an overlapping pair. A square object moves to the upper CCD and is captured by OA_1 to produce I_1, then the object moves to the lower CCD after a fixed time interval and is captured by OA_2 to produce I_2, the positions of the square object in I_1 and I_2 may be different due to $j_x(t)$ and $j_y(t)$.

Jitter estimation method takes advantage of two facts: the same object is imaged at slightly different times by an overlapping CCD pair and the same jitter affects all CCDs at the same time[14–16]. The relationship between jitter and position offset in overlapping image pairs can be expressed as

$$f(t) = j(t + \Delta t) - j(t), \tag{1}$$

where $f(t)$ is the position offset at time t, $j(t)$ is the jitter at time t, and $j(t+\Delta t)$ is the same jitter translated by time interval Δt. Transform it into frequency domain to obtain $F(f) = J(f) \cdot \exp(\mathrm{j}\,2\pi f \Delta t) - J(f)$, and simplify

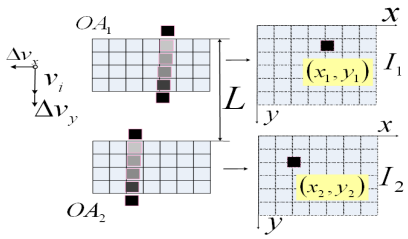

Fig. 1. Imaging process of the same object by the CCD overlapped areas.

the equation to get

$$J(f) = \frac{F(f)}{\exp(\mathrm{j}2\pi f\Delta t) - 1}. \quad (2)$$

Then $j(t)$ is obtained by calculating the inverse fractional transform of $j(f)$, but not all frequencies can be estimated, frequencies making the denominator in Eq. (2) zero cannot be estimated, in this case, exp (j2πfΔt) – 1 = 0, the unmeasurable jitter is defined as blind spot. $f^k = \frac{k}{\Delta t}, k = 0,1,2,\cdots, f^k$ is called as kth blind spot; the first blind spot is defined as basic frequency $F = \frac{1}{\Delta t}$, where $\Delta t = \frac{L \cdot a}{v_i + \Delta v_y}$, L is the number of lines (NLs) in space between two overlapping CCDs; a is the line width of CCD; v_i is the line speed, and $v_i = a/T_r = a \cdot F_r$, where T_r and F_r are imaging line time and line frequency of CCD; Δv_y is the unwanted velocity caused by jitter, v_i is usually much larger than Δv_y[17]. $|v_i| >> |\Delta v_y|$, then the time interval is simplified as $\Delta t = \frac{L \cdot a}{v_i + \Delta v_y} \approx \frac{L \cdot a}{v_i} = \frac{L \cdot a}{F_r \cdot a} = \frac{L}{F_r}$. Consequently, the basic frequency and kth blind spot can be expressed as

$$F = \frac{1}{\Delta t} = \frac{F_r}{L}, \quad (3)$$

$$f^k = kF = k\frac{F_r}{L}, k = 0,1,2,\cdots. \quad (4)$$

Blind spots are defined as the frequencies making the denominator in Eq. (2) zero. In practice, however, not only the exact blind spots but also such frequencies very near to blind spots that make the denominator close to zero cannot be estimated accurately either, the range near the k-th blind spot is called kth blind band.

$$\mathbf{B}^k = \varepsilon\left(f^k\right) = \varepsilon\left(kF\right) = \varepsilon\left(k\frac{F_r}{L}\right), k = 0,1,2,\cdots. \quad (5)$$

We eliminate blind bands in jitter estimation by improving the traditional layout of a focal plane. The focal plane is traditionally arranged with the configuration that all overlapping CCD pairs have the same distance (such as ASTER), but the existence of blind bands makes it not good enough for jitter estimation. We configure three parallel CCDs with two overlapping pairs (P_1 and P_2) and one non-overlapping pair (P_3), for the overlapping pairs, the NLs in space, basic frequencies, and blind bands are L_1, L_2, F_1, F_2, and $\varepsilon_1(k_1F_1)$, $\varepsilon_2(k_2F_2)$, (k_1, k_2 = 0, 1, 2, ...).

Blind frequencies aliasing will occur where two blind spots are overlapped or very close (the overlapping blind spots are called "common blind spots"), the maximum aliasing range occurs at common blind spots. All frequencies are divided into three groups: non-blind frequencies of both P_1 and P_2 (G_1); blind frequencies of either P_1 or P_2 (G_2); blind frequencies of both P_1 and P_2 (G_3). Jitter at frequencies in G_1 is determined by the average results of P_1 and P_2; that in G_2 (blind frequency of P_1 (P_2)) is estimated by the other pair P_2 (P_1); but the jitter in G_3 cannot be determined using the above method, this is what we mainly focus on. Since the maximum aliasing range occurs at common blind spots, our primary task is to minimize the number of common blind spots within bandwidth of jitter estimation. The solution is to make the two NLs L_1 and L_2 coprime numbers.

Here is the mathematical proof for the effect of coprime numbers. Assuming the minimal common blind spot, F_Σ, is the mth blind spot of F_1 and the nth of F_2 (m and n are positive integers), $F_\Sigma = mF_1 = nF_2$; then the kth common blind spots are $f_\Sigma^k = k \cdot F_\Sigma, k = 0,1,2,\cdots$. According to Eq. (3), $F_1 = F_r/L_1$; $F_2 = F_r/L_2$; so the line frequency F_r is a common blind spot, if it is also the minimal common blind spot, the number of common blind spots within F_r is minimized, and the number of common blind spots within bandwidth is also minimized (F_r is ~10 kHz, jitter estimation bandwidth is usually less than 10 kHz). Assuming F_r is the rth common blind spot (r is a positive integer), $F_r = r \cdot F_\Sigma$; then $m = \frac{F_\Sigma}{F_1} = \frac{F_r/r}{F_r/L_1} = \frac{L_1}{r}$, $n = \frac{F_\Sigma}{F_2} = \frac{F_r/r}{F_r/L_2} = \frac{L_2}{r}$ since L_1 and L_2 are coprime, the common divisor $r = 1$, then $F_\Sigma = F_r$, consequently, F_r is the minimal common blind spot. Therefore, the coprime numbers of L_1 and L_2 ensure to minimize the number of common blind spots within jitter estimation bandwidth.

The second task is to determine jitter at frequencies in G_3. The solution is to replace it with another pair whose blind bands do not cover G_3, since common blind frequencies may occur anywhere within jitter estimation bandwidth (Bw), we have to design a pair of CCD whose basic frequency should be greater than Bw, which requires very small distance between the CCD pair. However, current physical housings do not allow that small space between two partly overlapping CCDs, but we can access any small distance between two non-overlapping CCDs, which leads to a problem that no overlapping area means no overlapping images, no overlapping images means the offset between the pair cannot be obtained by image registration. We solve the problem by the following solutions. According to Eq. (1), the relationships between jitter and position offset in images of the above two overlapping pairs (P_1 and P_2) are

$$f_1(\tau) = s(\tau + \Delta t_1) - s(\tau); \tau \in \left[0, R - \Delta t_1\right], \quad (6)$$

$$f_2(\tau) = s(\tau + \Delta t_2) - s(\tau); t \in \left[0, R - \Delta t_2\right], \quad (7)$$

where $f_1(\tau)$ and $f_2(\tau)$ are the offset from P_1 and P_2, then

$$f_2(\tau) - f_1(\tau) = s(\tau + \Delta t_2) - s(\tau + \Delta t_1), \tau \in \left[0, R - \Delta t_2\right].$$

Let $f\left(\tau + \Delta t_1\right) = f_2(\tau) - f_1(\tau); \tau \in \left[0, R - \Delta t_2\right]$,

$t = \tau + \Delta t_1; \Delta t = \Delta t_2 + \Delta t_1; t \in \left[\Delta t_1, R - \Delta t\right]$, then

$$f(t) = s(t + \Delta t) - s(t); t \in \left[\Delta t_1, R - \Delta t\right]. \quad (8)$$

The indirect solution also increases systematic error of offset data. $\sigma = \sqrt{\sigma_1^{\,2} + \sigma_2^{\,2}}$,, where σ, σ_1, and σ_2 are the systematic errors of $f(t)$, $f_1(t)$, and $f_2(t)$. Although the error of offset by indirect method is greater than that by direct method, the final error is surely much less than the error of frequencies in G_3. Therefore, the function of the non-overlapping pair is to solve the common blind frequencies of the two overlapping pairs.

The line frequencies of all CCDs must be modulated at the same or different values to adapt to variation of orbital altitude or latitude for a space camera in flight. Our solutions for jitter estimation only applies for all CCDs (used for jitter estimation) working at the same line frequency, based on this idea, we suggest that the CCDs used for jitter estimation is set at the same line frequency. No matter how much the line frequencies of CCDs vary, the number and the times (kth) of common blind spots will not change, only the values of basic frequencies and common blind spots increase or decrease by the same amount with line frequencies. The parameters can be determined at the minimal line frequency and leave a certain margin, and then our solution is applicable for this case.

Here is the discussion on the influence of error on the NLs (L) in space. The relationship of error between basic frequency and L is $\sigma_F = \sigma_L \left|\frac{\partial F}{\partial L}\right| = \sigma_L \frac{F_r}{L^2}$, L usually ranges from hundreds to thousands, assuming $L = 1000$ lines; line frequency F_r is ~10 kHz and error of L, σ_L, is usually less than 0.5 lines. Based on the above equation, the error of basic frequency is ~0.005 Hz and the relative error is ~0.5%, which is insignificant.

Therefore, at least three CCDs with two overlapping and one non-overlapping pairs are needed for blind bands elimination. The NLs in space of the two overlapping pairs must be coprime numbers, and that of the non-overlapping pair must be less than the quotient of the minimal line frequency and the required jitter estimation bandwidth. Both the above conditions are realizable in practice.

A simulation model of jitter estimation assembly has been developed to validate the blind band elimination method. The relative motion is simulated by a moving target and a motion less camera, the moving target is an urban remote sensing image fixed to a vibration platform with a bandwidth of 0–60 Hz and the TDI camera is achieved by a CMOS array camera combined with digital domain TDI technology. The motion detected by a displacement sensor is regarded as the actual jitter with an accuracy of 5 μm, equal to 0.01 pixels; the jitter estimation algorithm is carried out by a computer.

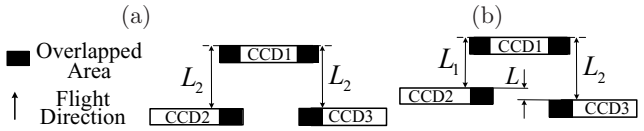

Fig. 2. Layout of three CCDs in the simulated TDI camera: (a) traditional layout and (b) improved layout.

Figure 2(b) shows the improved layout of focal plane for blind bands elimination in jitter estimation. Table 1 shows the parameters of the focal plane, the non-overlapping pair's space in along-track direction is set 1 line to be less than $Fr/B\omega = 240/60 = 4$ lines. The traditional layout with the same distance is designed as a control group (Fig. 2(a)).

Computer simulated results of both layouts are shown in Fig. 3 at line frequencies of (a) 315 and (b) 240 Hz (Fig. 3 only shows the maximal aliasing ranges in 0–60 Hz). The curves P_1 and P_2 represent relative standard deviations (STDs) of the two overlapping pairs. Frequencies are divided into three groups (G_1, G_2, and G_3) (bounded by the relative STD of 0.2): G_1, non-blind frequencies of both P_1 and P_2; G_2, blind frequencies of either P_1 or P_2; G_3, blind frequencies both P_1 and P_2.

We validate the effectiveness of the blind band elimination method by comparing the jitter measurement STD between the traditional and improved layouts of CCDs at G_1, G_2, and G_3; test the performance at variable line frequencies of CCDs by comparison of the STDs of G_1, G_2, and G_3 at different line frequencies (frame rate of CMOS array camera). Table 2 shows the frequency values chosen from the three groups with the same amplitude of 10 pixels.

Step 0: To calibrate the accuracy of vibration displacement sensor.

Step 1: Adjust the camera's exposure time.

Step 2: Set up the vibration parameters and start the vibration platform; start the camera and save images (call them I_1, I_2,...) after the vibration platform smooth working.

Step 3: Form simulated TDI images. Determine the TDI lines (N) according to image signal noise ratio, adding the first lines from I_1 to I_N together to form the first line of TDI image, and the same to others, we obtain TDI images of CCD1. The first image line of CCD2 is formed by adding the first lines from I_{L1+1} to $I_{L1+N.}$ Similarly, we get TDI images of CCD3.

Table 1. Parameters of the Focal Plane

Frame Rate (f/s)	$B\omega$ **(Hz)**	L_1 **(lines)**	F_1 **(Hz)**	L_2 **(lines)**	F_2 **(Hz)**	L **(lines)**	F **(Hz)**
315	60	35	9	36	8.75	1	315
240	60	35	6.86	36	6.67	1	240

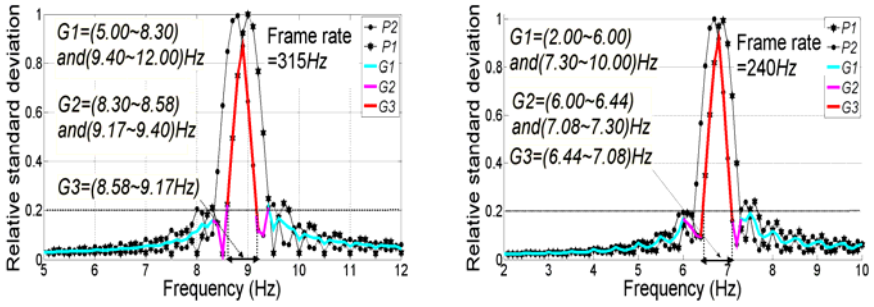

(a) (b)

Fig. 3. Simulation curve relative error against frequencies: frame rate equals (a) 315 and (b) 240 Hz. P_1, NL equals 36 lines; P_2, NL equals 35 lines; G_1, non-blind band of both P_1 and P_2; G_2, blind band of either P_1 or P_2; G_3, blind band of both P_1 and P_2.

Step 4: Estimate jitter matching overlapping images to obtain offset f_1, f_2; remove bad values and spline interpolate at the removed points; perform Fourier transform on the interpolated offset to obtain frequency-domain information of jitter according to Eq. (2). The jitter in time domain is obtained by inverse Fourier transform.

Step 5: Calculate STD of the difference between the measured jitter and the results by the vibration displacement sensor.

Figure 4 illustrates the differences between the actual jitter and the measured values of G_1, G_2, and G_3 at frame rates of 315 and 240 Hz, the broken and solid curves show the differences by the traditional and improved layout, respectively. When frame rate equals 315 Hz, the STD in group G_1 by the improved layout is 0.03 pixels less than that by the traditional layout (Fig. 4(a)), because the improved layout estimates jitter in G_1 using the average of two pairs, which reduces random noise. However the jitter estimated by the traditional layout only comes from one pair without weakening random noise. For the blind band G_2 (Fig. 4(c)), the traditional layout's STD is unacceptable, but the improved layout's STD, 0.46 pixels, is very close to that, 0.45 pixels, at non-blind frequencies in G_1, which proves that the improved layout works effectively at blind frequencies of one pair. For both pairs' blind band (G_3), the traditional layout's STD is extraordinarily large, compared with which, the improved layout's deviation, 0.61 pixels, is acceptable, but it is still 0.16 pixels larger than that at non-blind frequencies (G_1), because the subtraction of two pairs' offset data increased the error. The results in G_3 prove the effectiveness of the improved layout of CCDs at both pairs' blind frequencies. When frame rate equals 240 Hz, the STD (Figs. 4 (b), (d), or (f)) is very close to that at frame rate of 315 Hz, the effectiveness of the improved layout at different line frequencies of CCDs is also proved. Therefore, the improved layout of the CCDs can eliminate the blind bands within the bandwidth.

In conclusion, we propose the blind band elimination method based on an improved layout of focal plane. Three CCDs working at the same line frequency are required and designed with two pairs of overlapping area and one non-overlapping pair. Each pair of CCDs has a group of blind bands which are determined by the line frequency of CCDs and the NL in space of the pair. The two NLs of overlapping pairs are made coprime to minimize the number of common blind spots. The third non-overlapping pair is arranged with the space less than the quotient of the least line frequency and bandwidth, which aims at determining jitter at aliasing blind frequencies of the first two overlapping

Table 2. Results of the Vibration Experiments (TL, Traditional Layout and IL, Improved Layout)

Frame Rate (f/s)	**Frequency (Hz)**		**G_1**	**G_2**	**G_3**
315			5.0 + 12.0	8.4 + 9.3	8.6 + 9.0
	STD	TL	**0.48**	**2.91**	**5.99**
		IL	**0.45**	**0.46**	**0.61**
240	Frequency (Hz)		5.0 + 10.0	6.4 + 7.3	6.5 + 7.0
	STD	TL	**0.47**	**4.01**	**5.69**
		IL	**0.45**	**0.47**	**0.62**

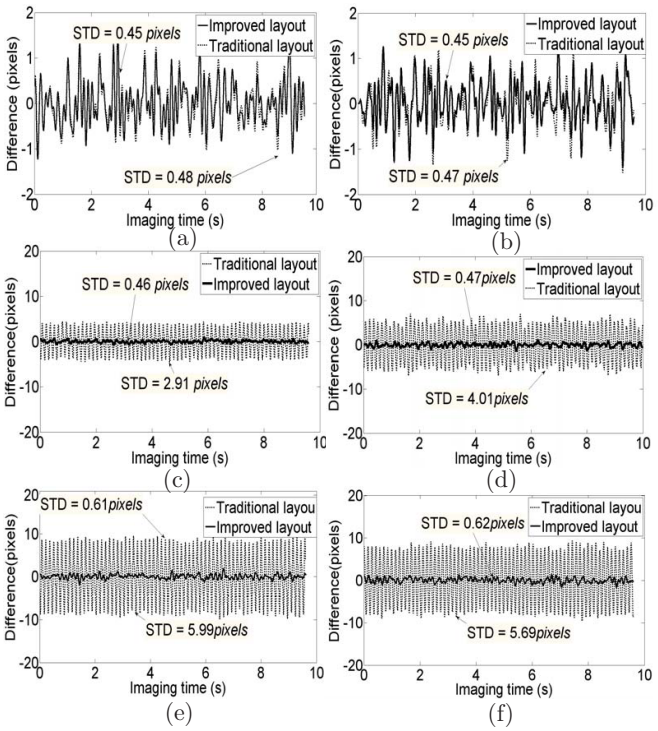

Fig. 4. Comparison of the jitter measurement STD between the traditional and improved layout of CCDs: G_1 at frame rate of 315 Hz, (b) G_1 at 240 Hz, (c) G_2 at 315 Hz, (d) G_2 at 240 Hz, (e) G_3 at 315 Hz, and (f) G_3 at 240 Hz.

pairs. Experimental results prove the effectiveness of non-zero blind band elimination in jitter estimation.

This work was assisted by Prof. Xu and all the engineers in the laboratory, with whose help the reasonable experimental results were obtained.

References

1. A. S. McEwen, M. E. Banks, N. Baugh, K. Becker, A. Boyd, J. W. Bergstrom, R. A. Beyer, E. Bortolini, N. T. Bridges, S. Byrne, B. Castalia, F. C. Chuang, L. S. Crumpler, I. Daubar, A. K. Davatzes, D. G. Deardorff, A. DeJong, W. A. Delamerei, E. N. Dobrea, C. M. Dundas, E. M. Eliason, Y. Espinoza, A. Fennema, K. E. Fishbaugh, T. Forrester, P. E. Geissler, J. A. Grant, J. L. Griffes, J. P. Grotzinger, V. C. Gulick, C. J. Hansen, K. E. Herkenhoff, R. Heyd, W. L. Jaeger, D. Jones, B. Kanefsky, L. Keszthelyi, R. King, R. L. Kirk, K. J. Kolb, J. Lasco, A. Lefort, R. Leis, K. W. Lewis, S. Martinez-Alonso, S. Mattson, G. McArthur, M. T. Mellon, J. M. Metz, M. P. Milazzob, R. E. Milliken, T. Motazedian, C. H. Okubo, A. Ortiz, A. J. Philippoff, J. Plassmann, A. Polit, P. S. Russell, C. Schaller, M. L. Searlsm, T. Spriggs, S. W. Squyres, S. Tarr, N. Thomas, B. J. Thomson, L. L. Tornabene, C. V. Houten, C. Verba, C. M. Weitz, and J. J. Wray Icarus **205,** 2 (2010).
2. A. S. McEwen, E. M. Eliason, J. W. Bergstrom, N. T. Bridges, C. J. Hansen, W. A. Delamere, J. A. Grant, V. C. Gulick, K. E. Herkenhoff, L. Keszthelyi, R. L. Kirk, M. T. Mellon, S. W. Squyres, N. Thomas, and C. M. Weitz J. Geophys. Res. **112,** E5 (2007).
3. R. Li, J. W. Hwangbo, and Y. H. Chen, IEEE Trans. Geosci. Remote Sens. **49,** 7 (2011).
4. W. A. Delamere, L. L. Tornabene, and A. S. McEwen, Icarus **205,** 38 (2010).
5. S. Mattson, R. Heyd, A. Fennema, R. Kirk, D. Cook, K. Becker, A. McEwen, and A. Boyd, in *Proceedings of European Planetary Science Conference* (2012).
6. S. S. Mattson, M. Robinson, A. McEwen, A. Bartels, E. Bowman-Cisneros, R. Li, J. Lawver, T. Tran, and K. Paris, in *Proceedings of 41nd Lunar and Planetary Science Conference* 1871 (2010).
7. S. S. Mattson, A. Bartels, A. Boyd, P. Calhoun, O. Hsu, A. McEwen, M. Robinson, J. Siskind, and T. Tran, in *Proceedings of 42nd Lunar and Planetary Science Conference* 2756 (2011).
8. T. Okuda and A. Iwasaki, in *Proceedings of IEEE Conference on IGARSS* (2010).
9. A. Iwasaki and H. Fujisada, Proc. SPIE **4881,** 111 (2003).
10. E. Zaunick, K. Janschek, and J. Levenhagen, in *Proceedings of 7th International ESA Conference on Guidance, Navigation & Control Systems* (2008).
11. K. Janschek, V. Tchernykh, and S. Dyblenko, in *Proceedings of IEEE Conference on Advance Intelligence Mechatronics* (2005).
12. K. Janschek and V. Tchernykh, in *Proceedings of 15th IFAC Symposium on Automatic Control in Aerospace* 127 (2001).
13. K. Janschek, V. Tchernykh, and S. Dyblenko, Control Eng. Pract. **15,** 3 (2007).
14. S. Mattson, A. Boyd, R. L. Kirk, D. A. Cook, and E. Howington-Kraus in *Proceedings of European Planetary Science Conference* 604 (2009).
15. Y. Teshima and A. Iwasaki, in *Proceedings of IEEE Conference on Geoscience Remote Sensor* (2008).
16. A. Iwasaki, in *Handbook of Advances in Spacecraft Technologies* J. Hall, ed. (InTech, 2011), pp. 257–272.
17. G. Hochmana, Y. Yitzhak1, N. S. Kopeika, Y. Z. Lauber, M. Citroen, and A. Stern, Proc. SPIE **5203,** 559 (2003).